Available online at www.sciencedirect.com
ScienceDirect
International Journal of Heat and Mass Transfer 51 (2008) 4862–4874
International Journal of HEAT and MASS TRANSFER
www.elsevier.com/locate/ijhmt

Nonequilibrium heat conduction in a nanofluid layer with periodic heat flux

Yuwen Zhang *, H.B. Ma

Department of Mechanical and Aerospace Engineering, University of Missouri, Columbia, MO 65211, USA

Received 19 June 2007; received in revised form 24 February 2008
Available online 12 April 2008

Abstract

Nonequilibrium heat conduction in a nanofluid layer with periodic heat flux on one side and specified temperature on the other side is studied numerically. The energy equations for the nanoparticles and base fluid are nondimensionalized and the problem is described by four dimensionless parameters: heat capacity ratio, volume fraction of nanoparticles, period of surface heat flux, and the Sparrow number. The Sparrow number is to describe the coupling between the energy equations for nanoparticles and base fluid. Nonequilibrium between nanoparticles and base fluid, as well as heat transfer enhancement in nanofluid, of three nanofluids (diamond–water, diamond–ethylene glycol, and copper–ethylene glycol) is investigated. The results showed that the nonequilibrium between the nanoparticles and base fluid exist for all three nanofluids at low Sparrow number and short period of surface heat flux. The results also showed that heat transfer in a liquid layer can be enhanced by adding nanoparticles to the base fluid, but the level of enhancement is not as high as those reported by using transient hot wire (THW) method.

1. Introduction

Nanofluid is produced by adding only a small amount of nanoparticles or nanotubes into the base fluid [1]. It was reported that a small amount (less than 1% volume fraction) of copper nanoparticles or carbon nanotubes dispersed in ethylene glycol or oil can increase their inherently poor thermal conductivity by 40% and 150%, respectively [2,3]. Das et al. [4] reported a 2–4-fold increase in thermal conductivity enhancement for water-based nanofluids containing Al_2O_3 or CuO nanoparticles over a small temperature range, 21–51 °C. Patel et al. [5] have shown a 5–21% increase in thermal conductivity of water at vanishing concentrations (<0.00026 vol%) of monosized gold nanoparticles with citrate stabilization. The synthesis, heat transfer mechanism, and applications of nanofluids have been thoroughly reviewed in Ref. [6,7].

Keblinski et al. [8] explored the possible factors influencing the heat transport capability of nanofluids that include: (1) Brownian motion of nanoparticles; (2) molecular-level layering of the liquid at the nanoparticle surface; (3) nature of heat transport in nanoparticles; and (4) the effects of nanoparticles clustering. An order of magnitude analysis showed that the Brownian motion of nanoparticles is too slow to transport significant amount of heat through a nanofluid; this conclusion was also supported by their results of molecular dynamics simulation. On the contrary, Kumar et al. [9] developed a model for heat conduction in nanofluids based on the assumption that Brownian motion of the nanoparticles is the leading cause of heat transfer enhancement. The mean free path of nanoparticle was assumed to be of the order of 1 cm, which led to significant contribution of Brownian motion on thermal transport in the nanofluids. Keblinski and Cahill [10] pointed out the contribution of Brownian motion on thermal transport in the nanofluids was overestimated by six orders of magnitude in Ref. [9], because the mean free path of the nanoparticles used by Kumar et al. [9] (~1 cm) was unrealistic and it should be equal to the size of the nanoparticles (~10 nm). Jiang and Choi [11] proposed a model for effective thermal conductivity of nanofluids by considering Brownian motion

* Corresponding author. Fax: +1 573 884 5090.
E-mail address: zhangyu@missouri.edu (Y. Zhang).

0017-9310/$ - see front matter © 2008 Elsevier Ltd. All rights reserved.
doi:10.1016/j.ijheatmasstransfer.2008.02.014

Nomenclature

c_p	specific heat [J/kg K]
C_{sf}	ratio of heat capacities of nanoparticles and base fluid
d_p	diameter of the nanoparticle [m]
G	coupling factor between nanoparticle and base fluid [W/m^3 K]
h_p	heat transfer coefficient at the nanoparticle surface [W/m^2 K]
k	thermal conductivity [W/m K]
L	thickness of the nanofluid layer
Nu	Nusselt number at nanoparticle surface
r_p	radius of the nanoparticle [m]
q''_0	amplitude of surface heat flux [W/m^2]
Sp	Sparrow number
t	time [s]
t_p	period of surface heat flux [s]
T	temperature [K]
x	coordinate [m]

Greek symbols

α	thermal diffusivity [m^2/s]
δ_{eq}	equivalent matrix thickness [m]
φ	volume fraction of nanoparticles
θ	dimensionless temperature
Θ	heat transfer enhancement parameter, Eq. (26)
ρ	density [kg/m^3]
τ	dimensionless time
τ_p	dimensionless period of surface heat flux

Subscripts

eff	effective
f	base fluid
i	initial
s	solid phase (nanoparticle)

of nanoparticles. Their model not only could capture the concentration and temperature-dependent conductivity, but also could predict the particle size dependent conductivity. Prasher et al. [12] pointed out that the model in Ref. [11] arbitrarily assumed that the thermal boundary layer on the nanoparticle is three times of the size of the base fluid molecules divided by the Prandtl number, and the assumption of parallel heat transfer mode by base fluid and nanoparticles was also not physically true for small volume fraction of nanofluids. Prasher et al. [12] developed an empirical correlation of the effective thermal conductivity by considering: (1) translational Brownian motion; (2) the existence of interparticle potential; and (3) convection in base fluid due to Brownian movement; their results agreed well with oxides nanoparticles. Evans et al. [13] analyzed the role of Brownian motion hydrodynamics on the thermal conductivity of the nanofluid by using a kinetic theory based analysis and molecular dynamics simulation; they concluded that the hydrodynamics effects associated Brownian motion have only minor effect on the thermal conductivity of the nanofluids. The viewpoints about the role of Brownian motion on the thermal conductivity of the nanofluids are still controversial at this time.

The atomic structure of liquid layer near the nanoparticle surface is significantly more ordered than that of the bulk liquid. Such liquid layering near the interface would have higher thermal conductivity, and Keblinski et al. [8] suggested that the liquid layering could contribute to higher thermal conductivity of the nanofluids. Xue [14] proposed a model based on the liquid layering theory with two adjustable parameters to match the experimental data: the thickness and thermal conductivity of the liquid layer. Xue and Xu [15] proposed a model of thermal conductivity of nanofluids with interfacial shells by considering the temperature distribution and liquid layering. They predicted the thermal conductivities of Al_2O_3/water, CuO/water, and CuO/ethylene glycol nanofluids using a 3-nm interfacial shell thickness and good agreement with experiments were obtained. Yu and Choi [16,17] developed a renovated Maxwell model and a renovated Hamilton–Crosser model for effective conductivity of nanofluids with spherical and nonspherical particles; they determined that the interfacial layer plays an important role on the enhanced thermal conductivity of nanofluids. Leong et al. [18] developed a model for the thermal conductivity of the nanofluid by solving 2D heat conduction in nanoparticle, solid-like interfacial layer, and fluid medium; they concluded that the interfacial layer is significant to enhancing the thermal conductivity of nanofluids. The shortcoming of the above models is that the liquid layering thickness cannot be determined by these models and must be obtained by matching the experimental data. The liquid layer thicknesses that is required to match with the experimental data are about 2–3 nm, which is significantly larger than the liquid thickness suggested by experiments [19] and molecular dynamics simulation [20] (3–5 times of the liquid molecular diameters). Xue et al. [20] suggested that the liquid layering was not responsible to the large enhancement of the nanofluid thermal conductivity. The role of liquid layering at the nanoparticle surface on the heat transfer enhancement is still debatable at this time.

The carrier of heat in the crystalline solid is phonon, i.e., propagation of lattice vibration. The commonly used diffusive heat transport theory is valid only if the mean free path of phonon is much less than the size of the crystalline solid. If the mean free path of the crystalline solid is comparable to or greater than the size of the crystalline solid, the diffusive heat transport mechanism is no longer valid and ballistic transport is more realistic. The mean free path of

phonon in Al_2O_3 at room temperature was 35 nm [8], which means that the phonon cannot diffuse in a nanoparticle with a diameter of 10 nm, and phonons must move ballistically in a nanoparticle. Keblinski et al. [8] suggested that a major increase of thermal conductivity can be expected if the ballistic phonons initiated in one nanoparticle can persist in the liquid and reach another nearby particle. The Brownian motion and liquid layering at the nanoparticle surface could potentially help the ballistic phonon motion from one nanoparticle to another. The role of ballistic phonon motion on the enhancement of thermal conductivity has received scant attention.

Another possible mechanism for enhancement of thermal conductivity is clustering of nanoparticles in the nanofluids, which could occur if the nanoparticles are not finely dispersed in the base fluid. Xuan et al. [21] pointed out that during stochastic motion of the suspended nanoparticles, aggregation and dispersion may occur among nanoparticle clusters and individual nanoparticles. Based on effective medium approximation and the fractal theory for the description of nanoparticle cluster and a radial distribution, Wang et al. [22] established a method for modeling the effective thermal conductivity of nanofluids. The role of nanoparticle clustering on the enhancement of the thermal conductivity needs further investigation.

The thermal conductivity of the nanofluids reported in the literature is usually obtained by using a well-established transient hot wire (THW) method. A very thin (5–80 μm in diameter) platinum or tantalum wire is embedded into the nanofluid and the thermal conductivity was obtained by measuring the rate of wire temperature change after a step voltage change is applied to it. Vadasz [23] investigated transient heat conduction in a nanofluid with an embedded hot wire using the dual-phase lagging (DPL; [24]) model. The results showed that an apparent effective thermal conductivity enhancement of the same quantitative values as the experiments suggested can be obtained if the DPL led by the solid–liquid interface heat transfer mechanism is accounted for. Recently, Putnam et al. [25] reported an optical beam deflection technique for measurement of thermal diffusivity of the nanoparticles; they did not observe anomalous enhancements of the thermal conductivity that was reported previously. Evans et al.'s theoretical work [13] also suggested that thermal conductivity of a nanofluid with *well dispersed* nanoparticles can be well described by the effective medium theory and did not show any significant enhancements.

Thin film evaporation and condensation can find their applications in many two-phase devices, such as heat pipes and fuel cells. Oscillating or pulsating heat pipes (OHP or PHP) are a new two-phase heat transfer device that can transfer heat via thermally excited oscillatory flow of the working fluid [26]. When the liquid slugs move back and forth in an OHP, a thin liquid film will be left behind on the inner wall. Evaporation and condensation over this thin liquid film contribute to oscillatory flow and heat transfer in an OHP [27]. Most recently, we charged the nanofluid (HPLC grade water containing 1.0 vol% 5–50 nm of diamond nanoparticles) into an OHP and found that nanofluids significantly enhance the heat transport capability in the OHP [28,29]. When the power input added on the evaporator is 100 W, the temperature difference between evaporator and condenser can be reduced from 42 to 25 °C by addition of nanoparticles.

Motivating by the application of nanofluid in OHP and other two-phase devices, heat transfer conduction across a thin nanofluid film subject to periodic heat flux heating on one side and specified temperature on the other side will be investigated in this paper. The conditions under which non-equilibrium between nanoparticles and base fluid exits will be identified; the effects of the nanoparticles on the heat conduction of nanofluid layer will be investigated.

2. Physical model

The physical model of the problem under consideration is shown in Fig. 1. A nanofluid layer with a thickness of L and an initial temperature of T_i is subjected to a periodic heat flux at one side and the temperature other side is kept at constant, T_i. It is assumed that heat transfer is 1D along the thickness of the nanofluid layer and the natural convection is neglected because the nanofluid layer is very thin. When the nanofluid layer is heated ($q'' > 0$), heat is transferred to the base fluid first and then the nanoparticles are heated by the base fluid. On the other hand, when the nanofluid layer is cooled ($q'' < 0$), the base fluid is cooled first and the nanoparticles are then cooled by interaction with the base fluid. For the physical model shown in Fig. 1, it is expected that there will be a delay from the variation of the temperature of the base fluid to that of the nanoparticles. In this work, the nonequilibrium between the nanoparticles and the base fluid will be modeled using a two-temperature model [30]. The energy equations of the nanoparticles (s) and the base fluid (f) can be, respectively, expressed as

$$\varphi(\rho c_p)_s \frac{\partial T_s}{\partial t} = G(T_f - T_s) \tag{1}$$

$$(1-\varphi)(\rho c_p)_f \frac{\partial T_f}{\partial t} = k_{eff} \frac{\partial^2 T_f}{\partial x^2} + G(T_s - T_f) \tag{2}$$

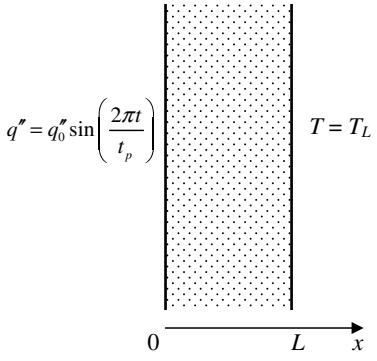

Fig. 1. Physical model.

where k_{eff} is the effective thermal conductivity of the nanofluid, and G is the coupling factor between the nanoparticles and the base fluid. The spatial derivative of the nanoparticle temperature did not appear in Eq. (1) because nanoparticles are dispersed in the base fluid and the interaction between different nanoparticles can be achieved through the base fluid only [23]. Patel et al. [31] also assumed that there is no direct interaction between nanoparticles in their latest work on a cell model approach for thermal conductivity of nanofluids. Eq. (1) indicates that the thermal conductivity of the nanoparticle material is irrelevant to the heat transfer of the nanofluid, but the heat capacity of the nanoparticle material, $(\rho c_p)_s$, is important because it dictates the nanoparticle temperature change. It should be pointed out that the above statement on irrelevance of the thermal conductivity of particle on the heat transfer in nanofluid is based on the assumption that there is no interaction (collision) between particles [there is no diffusion term in Eq. (2)]. For the case that the conductivity of nanoparticle material is higher or high volume fraction of nanoparticles, the interaction between the particles may become important and Eq. (1) may need to be modified.

The initial conditions of the problem are

$$T_s(x,0) = T_f(x,0) = T_i \tag{3}$$

The boundary conditions are

$$-k_{eff}\left.\frac{\partial T_f}{\partial x}\right|_{x=0} = q_0'' \sin\left(\frac{2\pi t}{t_p}\right), \quad x = 0 \tag{4}$$

$$T_f = T_i, \quad x = L \tag{5}$$

In arriving to Eq. (4), it is assumed that the heat flux goes first to the liquid and then to the nanoparticles. This assumption is valid because the volume fraction of the nanoparticle is very low and the number of nanoparticles in touch with the surface will be even lower. In addition, the Brownian motion of nanoparticles will make the time that a nanoparticle is in contact with the surface very short.

Defining the following dimensionless variables

$$\theta = \frac{k_f(T - T_i)}{q_0'' L}, \quad X = \frac{x}{L}, \quad \tau = \frac{\alpha_f t}{L^2} \tag{6}$$

Eqs. (1)–(5) become

$$C_{sf}\frac{\partial \theta_s}{\partial \tau} = Sp(\theta_f - \theta_s) \tag{7}$$

$$(1-\varphi)\frac{\partial \theta_f}{\partial \tau} = K_{eff}\frac{\partial^2 \theta_f}{\partial X^2} + \varphi Sp(\theta_s - \theta_f) \tag{8}$$

$$\theta_s(X,0) = \theta_f(X,0) = 0 \tag{9}$$

$$-K_{eff}\left.\frac{\partial \theta_f}{\partial X}\right|_{X=0} = \sin\left(\frac{2\pi\tau}{\tau_p}\right), \quad X = 0 \tag{10}$$

$$\theta_f = 0, \quad X = 1 \tag{11}$$

where

$$C_{sf} = \frac{(\rho c_p)_s}{(\rho c_p)_f} \tag{12}$$

$$K_{eff} = \frac{k_{eff}}{k_f} \tag{13}$$

$$Sp = \frac{GL^2}{\varphi k_f} \tag{14}$$

are the heat capacity ratio between nanoparticle and base fluid, dimensionless effective thermal conductivity of the nanofluid, and Sparrow number [32], respectively. In order to isolate the effects of the volume fraction of the nanoparticles, all of the dimensionless variables in Eqs. (6), (13) and (14) have been defined based on the properties of the base fluid. Assuming that the nanoparticles are well dispersed in the base fluid and the dimensionless effective thermal conductivity can be described by effective media theory [13,33], i.e.,

$$K_{eff} = 1 + 3\varphi\frac{\gamma - 1}{\gamma + 2} \tag{15}$$

where

$$\gamma = \frac{r_p}{\delta_{eq}} \tag{16}$$

and r_p is radius of the nanoparticles, and δ_{eq} is the equivalent matrix thickness – defined as a ratio of thermal conductance at the interface between the nanoparticles and the base fluid and thermal conductivity of the base fluid [33]. When the interfacial resistance nanoparticle surface is negligible, δ_{eq} becomes very small, which leads to $\gamma \to \infty$. In this case, Eq. (15) is reduced to

$$K_{eff} = 1 + 3\varphi \tag{17}$$

The nanoparticle–base fluid coupling factor, G, appeared in Eqs. (1) and (2) is an very important property of the nanofluid that dictates energy exchange between the nanoparticles and base fluid. If it is assumed that the Newton's law of cooling can be used to describe heat transfer between the nanoparticles and the base fluid, the coupling factor can be determined by

$$G = \frac{\varphi A_p h_p}{V_p} \tag{18}$$

where h_p is the heat transfer coefficient at the nanoparticle surface, A_p is the surface area of nanoparticle, and V_p is the volume of the nanoparticle. In Eq. (18), $\varphi A_p/V_p$ represents the specific interfacial area (m^2/m^3), i.e., the interfacial area between the nanoparticles and base fluid per unit volume of the nanofluid. If the nanoparticle is spherical in shape, this surface-area-to-volume ratio become $6\varphi/d_p$ where d_p is the diameter of the nanoparticle. For a nanofluid contains 1% of nanoparticle with $d_p = 10$ nm, the specific interfacial area is $6 \times 10^6\ m^2/m^3$! For the nanofluid with spherical nanoparticles, Eq. (18) becomes

$$G = \frac{6\varphi h_p}{d_p} \tag{19}$$

Substituting Eq. (19) into Eq. (14), the Sparrow number becomes

$$Sp = 6\frac{Nu}{K_{\text{eff}}}\left(\frac{L}{d_{\text{p}}}\right)^2 = 6\frac{Nu}{(1+3\varphi)}\left(\frac{L}{d_{\text{p}}}\right)^2 \tag{20}$$

where the Nusselt number is defined as

$$Nu = \frac{h_{\text{p}} d_{\text{p}}}{k_{\text{eff}}} \tag{21}$$

Eq. (20) is based on the assumption that the Newton's law of cooling is valid at the nanoscale. If this is a valid assumption and heat exchange between the nanoparticles and base fluid is by conduction only, the Nusselt number is in Eq. (20) will be equal to 2 and the Sparrow number will be inversely proportional to d_{p}^2. However, as the heat transfer in the nanoparticle is ballistic rather than diffusive, the validity of the Newton's law of cooling becomes questionable at the nanoparticle surface. Since ballistic heat transfer is not as effective as diffusive heat transfer, Vadasz [23] suggested that the heat transfer coefficient, h_{p}, may be reduced by several orders of magnitude and this reduction may result in a lower coupling factor. While there is very little effect on determining the coupling factor [23], Eq. (20) qualitatively demonstrated that Sparrow number depends on the heat transfer between the nanoparticles and base fluid, volume fraction of nanoparticles, and the ratio of the nanofluid layer thickness and diameter of the nanoparticles. In stead of attempting to uncover the roles of these individual factors, their collective effects on the nonequilibrium heat conduction in the nanofluid is represented by a single dimensionless parameter – Sparrow number – in the dimensionless governing equations.

While Eqs. (7) and (8) can be easily solved numerically, the dual phase lagging behavior of nanofluid can be examined by combining Eqs. (7) and (8) to eliminate the nanoparticle temperature, i.e.,

$$\tau_q \frac{\partial^2 \theta_{\text{f}}}{\partial \tau^2} + \frac{\partial \theta_{\text{f}}}{\partial \tau} = \bar{\alpha}_{\text{eff}}\left[\frac{\partial^2 \theta_{\text{f}}}{\partial X^2} + \tau_T \frac{\partial^2}{\partial X^2}\left(\frac{\partial \theta_{\text{f}}}{\partial \tau}\right)\right] \tag{22}$$

where

$$\bar{\alpha}_{\text{eff}} = \frac{K_{\text{eff}}}{(1-\varphi)+\varphi C_{\text{sf}}} \tag{23}$$

is the dimensionless effective thermal diffusivity of the nanofluid, and

$$\tau_q = \frac{(1-\varphi)}{[(1-\varphi)/C_{\text{sf}}+\varphi]Sp} \tag{24}$$

$$\tau_T = \frac{C_{\text{sf}}}{Sp} \tag{25}$$

are heat flux and temperature related dimensionless time lags in the dual-phase lagging model. It can be seen from Eqs. (24) and (25) that both τ_q and τ_T increase with increasing C_{sf} and decreasing Sp. Therefore, the dual-phase lagging behavior of the nanofluid will be more pronounced with higher C_{sf} and lower Sp, which will be conformed in the computational results. Comparison between τ_q and τ_T defined in Eqs. (24) and (25) also indicates $\tau_T > \tau_q$ for nanofluid, which is in agreement with Ref. [23].

The solution of Eqs. (7) and (8) is equivalent to that of Eq. (22). While the former focuses on the non-equilibrium between the nanoparticles and the base fluid, the latter focuses on the dual-phase lagging behavior caused by the nonequilibrium in the nanofluid. Therefore, the conditions under which the nonequilibrium exists in the nanofluid will also be the conditions that the nanofluid exhibits dual-phase lagging behavior. It should be pointed out that the dual-phase lag behavior shown in Eq. (22) is based on the assumptions made in forming Eqs. (1) and (2). More experimental evidences through measurement of the two relaxation times will be needed to unveil the dual-phase lag behavior. In this paper, the numerical solution of Eqs. (7) and (8) will be obtained, and the effects of various parameters on the nonequilibrium and the heat transfer of nanofluid will be discussed.

3. Numerical solution

The heat conduction in the nanofluid layer subject to periodic heat flux has been modeled using a two-temperature model. Heat transfer in nanoparticles and base fluid is coupled and therefore an iteration is needed to obtain the solutions of the two temperatures. The governing equations for heat transfer in nanofluid are similar to those encountered in heat transfer in porous media [30,34,35] or microscale heat transfer [36]. Eq. (8) is discretized using an implicit scheme [37] and the resulting algebraic equations are solved using tri-diagonal matrix algorithm (TDMA). After the grid number and time step independent tests, the grid number for all computations is 502 with a time step of $\Delta\tau = \tau_{\text{p}}/200$. The numerical solution for each time step begins with solution of the nanoparticle temperature, θ_{s}, from Eq. (7) based on an assumed base fluid temperature distribution, θ_{f}. The nanoparticle temperature is then used to obtain the updated base fluid temperature $\theta_{\text{f}}^{\text{new}}$ from Eq. (8), which is then compared with the assumed base fluid temperature, θ_{f}. If the maximum difference between $\theta_{\text{f}}^{\text{new}}$ and θ_{f} is less than a small tolerance value, 10^{-10}, end the iteration for the current time step and go to the next time step. Otherwise, update θ_{f} and repeat the iteration until the convergence criterion is met. Underrelaxation is not necessary during the iteration.

After several periods of surface heat flux, steady oscillation will be established and the dimensionless heating surface temperature of fluid will oscillate between a maximum value, $\theta_{\text{f,max}}$, and a minimum $\theta_{\text{f,min}}$. If heat transfer is enhanced by adding nanoparticles into the base fluid, it is expected that the difference between $\theta_{\text{f,max}}$ and $\theta_{\text{f,min}}$ for nanofluid will be smaller than that of the pure fluid. Thus, one can define the following parameter as a measure of the heat transfer enhancement

$$\Theta = \frac{(\theta_{f,\max} - \theta_{f,\min})|_{X=0,\varphi=0}}{(\theta_{f,\max} - \theta_{f,\min})|_{X=0,\varphi>0}} - 1 \quad (26)$$

Effects of various dimensionless parameters on nonequilibrium between nanoparticles and base fluid, and the heat transfer enhancement due to addition of nanoparticles, will be investigated in this paper.

4. Results and discussions

Heat conduction in a nanofluid layer described by Eqs. (7), (8), (9), (10), (11) and (17) is dominated by four dimensionless parameters: the ratio of heat capacities of nanoparticles and base fluid, C_{sf}, volume fraction of nanoparticles, ϕ, Sparrow number, Sp, and dimensionless period of the surface heating, τ_p. The ratio of the heat capacities of nanoparticles and base fluid, C_{sf}, depends on the combination of nanoparticle materials and the type of base fluid. The ratios of heat capacities of commonly used nanoparticles and base fluid are tabulated in Table 1. It can be seen that the ratio of heat capacity can vary over one order of magnitude. In this work, nonequilibrium between nanoparticles and base fluid for three different nanofluids (diamond nanoparticles dispersed in water or ethylene glycol, or copper nanoparticles dispersed in ethylene glycol) will be investigated. These three different nanofluids are chosen because their C_{sf} spread over the entire range in Table 1. The Sparrow number is a very important measure of nanoparticles–base fluid interaction. While the exact value of Sparrow number under different condition is unknown, Eq. (20) can provide an upper bound of the Sparrow number. Based on the size of nanoparticles commonly used in nanofluid and the thickness of the liquid film used in heat pipes and other two-phase devices, the Sparrow number used in this work is 500 and 1000.

Fig. 2 shows the effect of the dimensionless period of surface heat flux, τ_p, on the temperature of nanoparticles and base fluid of diamond–water nanofluid ($C_{sf} = 0.443$) at the heating surface ($X = 0$). The surface temperatures for the fluid with 2% nanoparticles and without nanoparticles ($\varphi = 0\%$) were plotted in Fig. 2. It can be seen that the oscillations of the surface temperature lag the oscillations of surface heat flux for both $\varphi = 2\%$ and $\varphi = 0\%$. When $\tau_p = 0.001$, the amplitude of the nanoparticle temperature is significantly smaller than that of the base fluid – indicating severe nonequilibrium between nanoparticles and the base fluid. As τ_p increases from 0.001 to 0.1, the amplitude of nanoparticle temperature oscillation becomes closer to that of the base fluid. When τ_p is 0.1, the amplitudes of temperature oscillation for nanoparticles and base fluid become very close, i.e., equilibrium between nanoparticles and base fluid is reached for $\tau_p = 0.1$. Since heat is transferred to base fluid first and the nanoparticle temperature can be changed by coupling with base fluid only [see Eq. (7)], the oscillation of nanoparticle temperature always lags behind the oscillation of base fluid temperature. The time

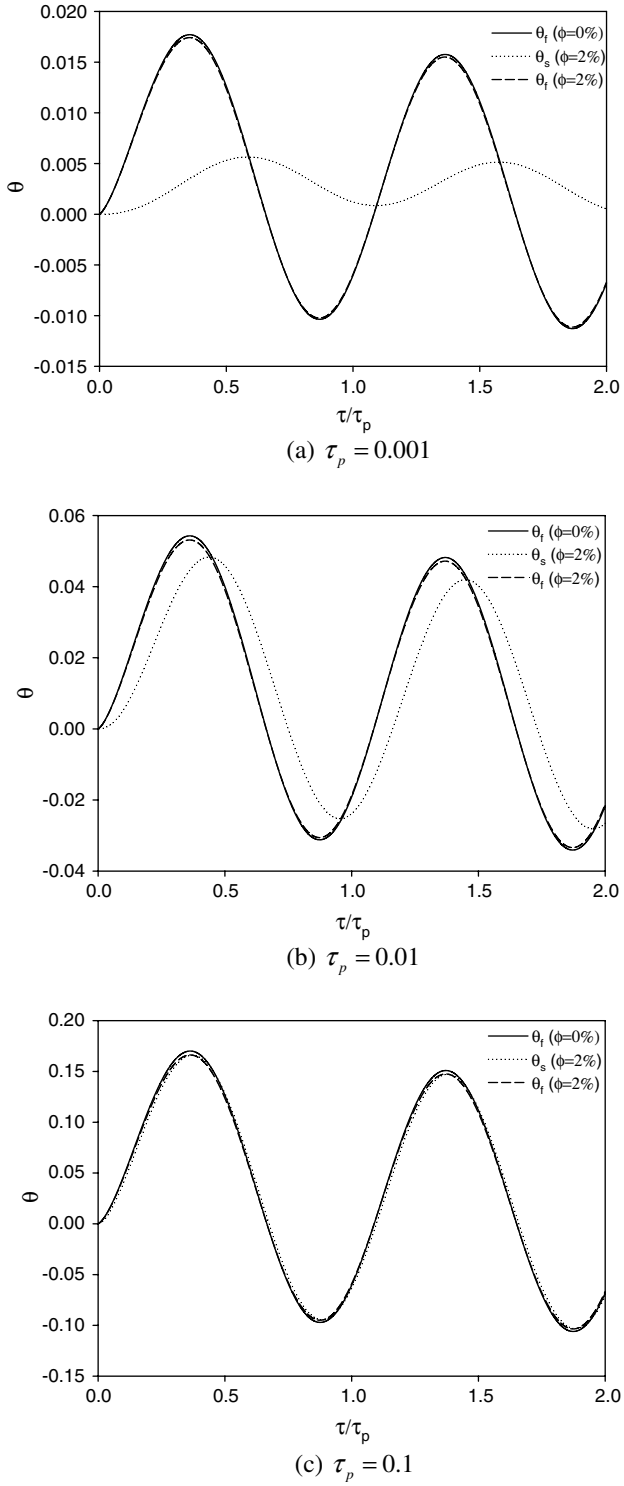

Fig. 2. Surface temperature for diamond–water nanofluid ($C_{sf} = 0.443$, $Sp = 500$, $\varphi = 2\%$).

Table 1
Ratio of heat capacities of selected nanoparticles and base fluid

C_{sf}	Diamond	Al_2O_3	CuO	Copper
Water	0.443	0.751	0.780	0.852
Ethylene glycol	2.728	4.624	4.804	5.248

delay from the base fluid temperature oscillation to the nanoparticle temperature oscillation decreases as τ_p increases. When τ_p is 0.1, the phases of temperature oscillation for nanoparticles and base fluid are nearly identical. For all three periods of surface heat fluxes shown in Fig. 2, the effects of nanoparticle on the fluid temperatures are very insignificant. The heat transfer enhancement parameter, Θ, for the three cases are 1.14%, 2.14% and 2.34%, respectively.

To investigate the effect of volume fraction of the nanoparticles on the nonequilibrium and heat transfer, simulation is performed for $\phi = 5\%$ and the results are shown in Fig. 3. All other parameters are kept the same as those used in Fig. 2. The trends on nonequilibrium between nanoparticles and base fluid are similar to those at lower volume fraction of nanofluid: nonequilibrium between nanoparticle and base fluid is pronounced for the cases with short τ_p and equilibrium between nanoparticles and base fluid is achieved for longer τ_p. The effects of nanoparticle on the surface temperature for the cases with 5% nanoparticles are more significant than that of $\varphi = 2\%$. The heat transfer enhancement parameter, Θ, for the three different periods of surface heat fluxes are 3.49%, 5.18% and 5.66%, respectively.

The results presented in Figs. 2 and 3 did not exhibit anomalous enhancement of heat transfer in nanofluids. To further study the heat transfer characteristics of diamond–water nanofluid under periodic heat flux, numerical simulation is performed for the cases with Sparrow number equal to 1000 (while all other parameters are kept the same as those used in Fig. 3) and the results are shown in Fig. 4. When $\tau_p = 0.001$, the amplitude of the oscillation of the nanoparticle temperature significantly increases with increasing Sparrow number. The phase difference between the oscillation of the nanoparticle temperature and base fluid temperature also decreases as Sparrow number increases. When $\tau_p = 0.01$, the increase of amplitude of the oscillation of the nanoparticle temperature and decrease of the phase difference between θ_s and θ_f are apparent although they are not as significant as for the case of $\tau_p = 0.001$. When the period is further increased to 0.1, increasing Sparrow number did not have any significant effect on the nonequilibrium between the nanoparticles and the base fluid because equilibrium is already reached at $Sp = 500$. The heat transfer enhancement parameter, Θ, for the three different periods of surface heat fluxes are same as those for the case of $Sp = 500$. Thus, increasing Sparrow number has effects on the nonequilibrium in the diamond–water nanofluid but its effect on heat transfer enhancement is negligible for the pure conduction of nanofluid.

Heat conduction in nanofluid formed by dispersing diamond nanoparticles into ethylene glycol (EG) is simulated next. Effects of τ_p on the nanoparticles and base fluid temperature at $X = 0$ for $\varphi = 0\%$ and 2% are shown in Fig. 5. When the dimensionless τ_p is 0.001, the nanoparticle temperature is almost unchanged when the base fluid temperature oscillates. The reason for the slow reaction of the nanoparticle temperature is that the heat capacity ratio for diamond–EG nanofluid, $C_{sf} = 2.728$, is much higher than that of diamond–water nanofluid (0.443) and the same level of energy exchange between nanoparticles and base fluid will result in slower change on the nanoparticle

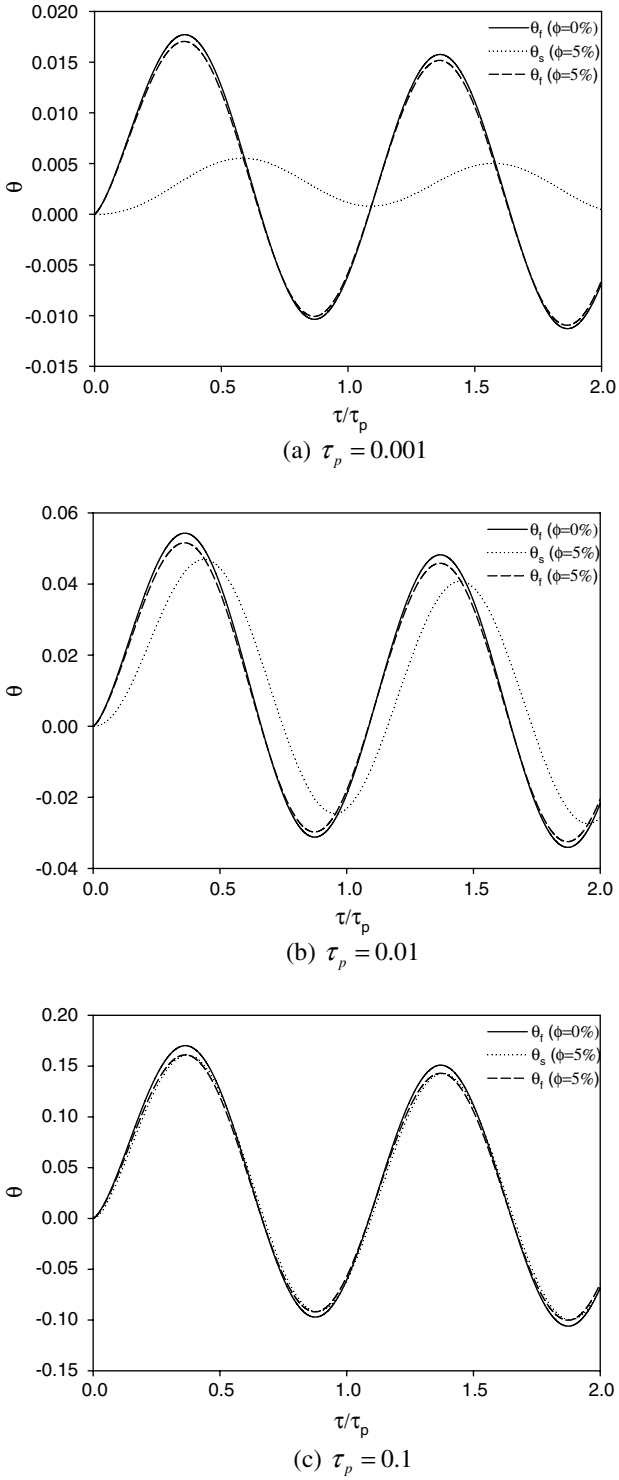

Fig. 3. Surface temperature for diamond–water nanofluid ($C_{sf} = 0.443$, $Sp = 500$, $\varphi = 5\%$).

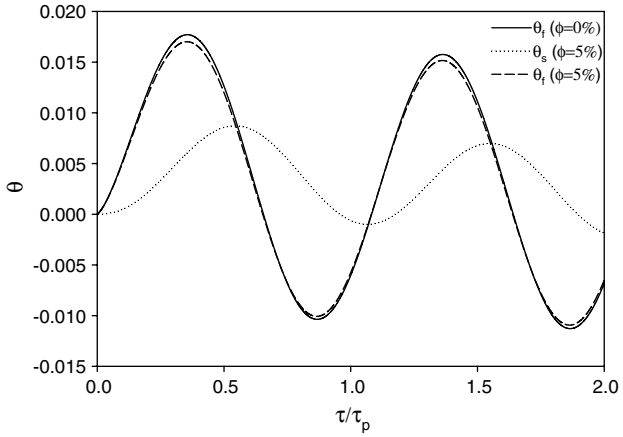

(a) $\tau_p = 0.001$

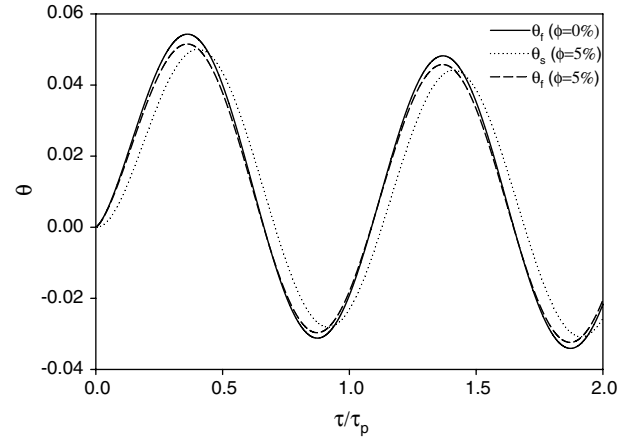

(b) $\tau_p = 0.01$

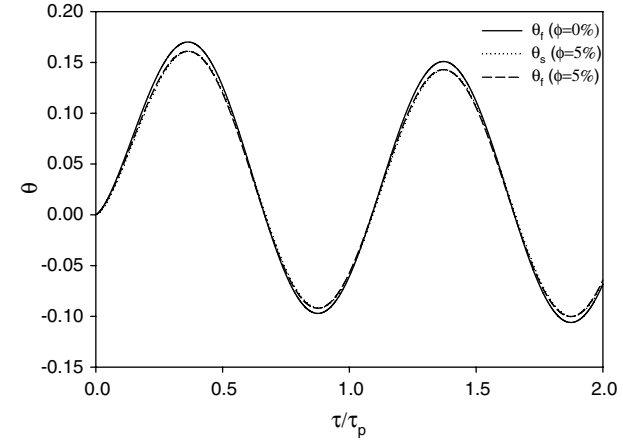

(c) $\tau_p = 0.1$

Fig. 4. Surface temperature for diamond–water nanofluid ($C_{sf} = 0.443$, $Sp = 1000$, $\varphi = 5\%$).

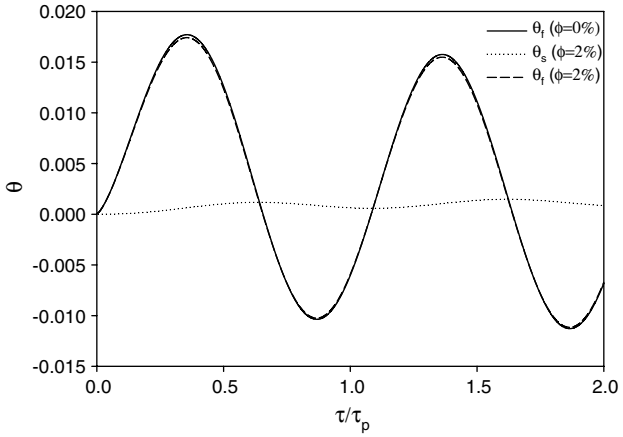

(a) $\tau_p = 0.001$

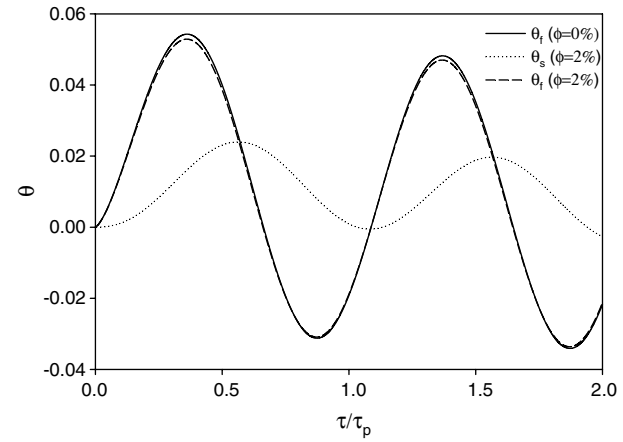

(b) $\tau_p = 0.01$

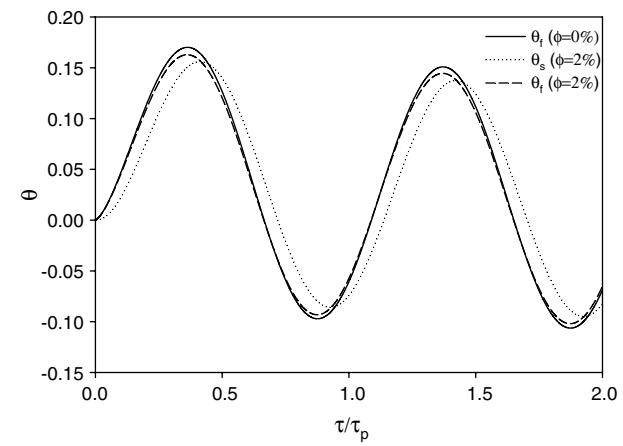

(c) $\tau_p = 0.1$

Fig. 5. Surface temperature for diamond–EG nanofluid ($C_{sf} = 2.728$, $Sp = 500$, $\varphi = 2\%$).

temperature. For $\tau_p = 0.01$, the amplitude of nanoparticle temperature oscillation is also much lower than that for the diamond–water nanofluid due to its large heat capacity ratio. Comparing Figs. 2 and 5b indicates that the phase lag between the base fluid and nanoparticle temperature also increases with increasing C_{sf}. When τ_p is increased to 0.1, the nanoparticles and base fluid still did not reach to equilibrium. The difference on the amplitudes of the oscillation temperature of the nanoparticles and base fluid, as well as phase lag from base fluid temperature to nanoparticle temperature, is still noticeable. It can be concluded from comparison between Figs. 2 and 5 that

nonequilibrium phenomenon is more pronounced for nanofluid with higher heat capacity ratio, C_{sf}. The heat transfer enhancement parameter, Θ, for the diamond–EG nanofluid with 2% nanoparticle for the three cases studied in Fig. 5 are 1.52%, 2.01% and 4.36%, respectively. The effect of C_{sf} on heat transfer enhancement parameter for $\tau_p = 0.001$ and 0.01 are negligible, but its effect for $\tau_p = 0.1$ is significant.

Fig. 6 shows the temperature oscillation of nanoparticles and base fluid for $\phi = 5\%$ while all other parameters are kept the same as those used in Fig. 5. Compared with the results in Fig. 5, the differences between θ_f with and without nanoparticles are more significant. The nonequilibrium in the diamond–EG nanofluid shown in Fig. 6 are also more significant than those for the diamond–water nanofluid exhibited in Fig. 3. The heat transfer enhancement parameter, Θ, for the three different periods of surface heat fluxes are 3.49%, 4.77% and 10.88%, respectively. Compared to the case with 2% nanoparticles, the heat transfer enhancement parameter for all three periods of surface heat flux, especially for $\tau_p = 0.1$, are significantly increased with increasing ϕ. Compared with the diamond–water nanofluid, the heat transfer enhancement parameter of the diamond–EG nanofluid for $\tau_p = 0.001$ and 0.01 did not show any difference; however, the heat transfer enhancement for $\tau_p = 0.1$ increases significantly.

The heat transfer characteristics of diamond–EG nanofluid is further investigated for the case with $Sp = 1000$ and the results are plotted in Fig. 7. The amplitudes of the temperature oscillation of the nanoparticles increase with increasing Sparrow number for all three periods of surface heat flux. The phase difference between the temperature oscillations of the nanoparticles and base fluid decreases with increasing Sparrow number noticeably. The heat transfer enhancement parameter, Θ, for the three different periods of surface heat fluxes are 3.49%, 6.14%, and 11.41%, which is very close to the values for the case of $Sp = 500$, i.e., the effect of the Sparrow number on heat transfer enhancement is very insignificant.

The third nanofluid investigated in this paper is formed by dispersing copper nanoparticles into ethylene glycol (EG), which yields a very high heat capacity ratio of 5.248. Fig. 8 shows the temperature oscillations of the nanoparticles and base fluid at the heating surface ($X = 0$) for $\varphi = 0\%$ and 2%. The amplitudes of nanoparticle temperature oscillation for all three periods of surface heat flux are lower than those for the diamond–EG nanofluid under the same conditions because the heat capacity ratio of copper–EG nanofluid is twice of that of diamond–EG nanofluid (2.728). The phase lags between the base fluid and nanoparticle temperatures for copper–EG nanofluid are also longer than those of diamond–EG nanofluid due to increased C_{sf}. The trends in Figs. 2, 5 and 8 demonstrated that increasing heat capacity ratio causes more significant nonequilibrium in the nanofluid. For the three cases studied in Fig. 8, the heat transfer enhancement parameter, Θ, are 1.52%, 1.88% and 5.62%, respectively. It can be seen that doubling C_{sf} has little effect on the heat transfer enhancement parameter for $\tau_p = 0.001$ and 0.01, and heat transfer for $\tau_p = 0.1$ is slightly enhanced.

Simulation is then carried out for the cases with volume fraction of nanoparticles equal to 5% (while all other parameters are unchanged) and the results are plotted in

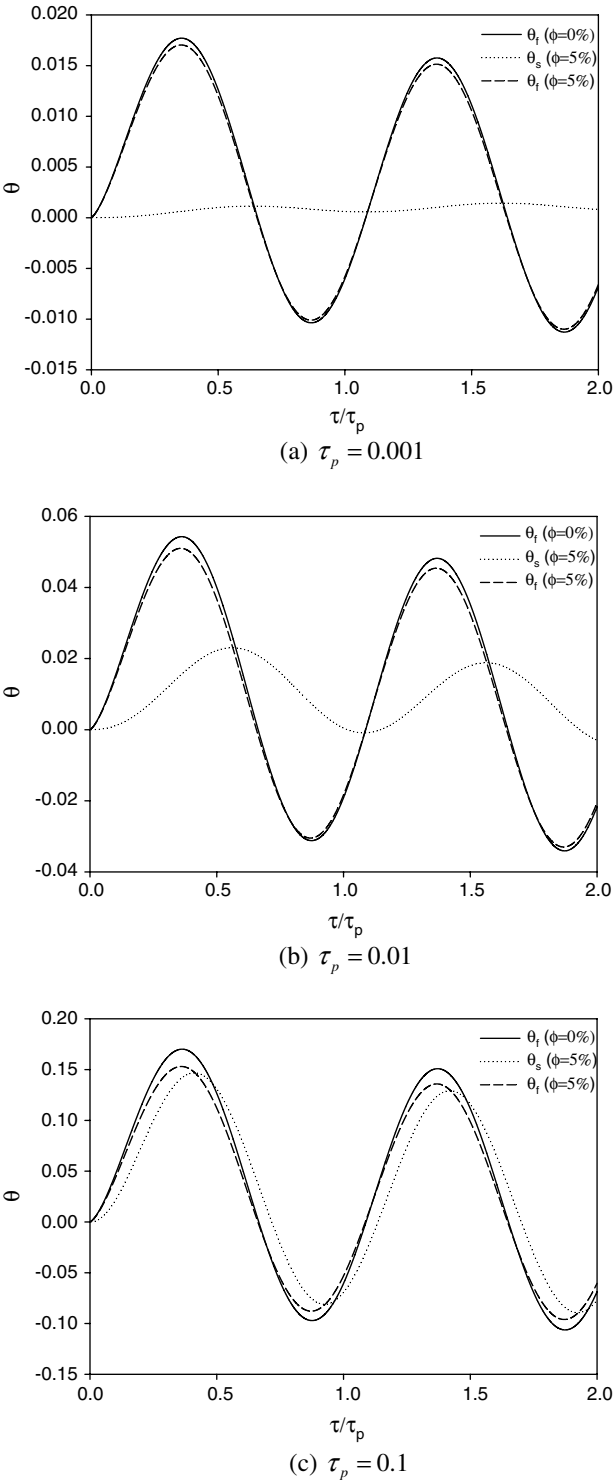

Fig. 6. Surface temperature for diamond–EG nanofluid ($C_{sf} = 2.728$, $Sp = 500$, $\varphi = 5\%$).

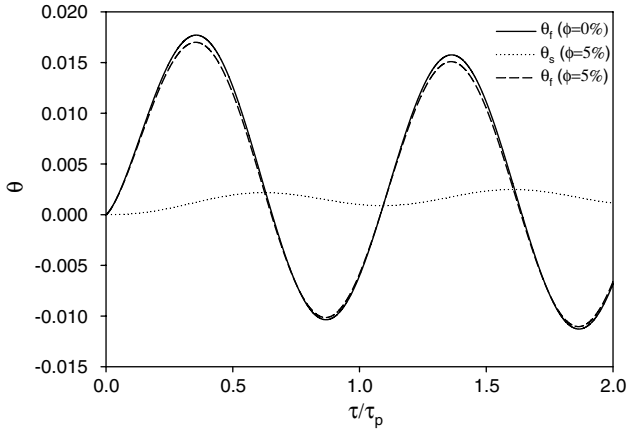

(a) $\tau_p = 0.001$

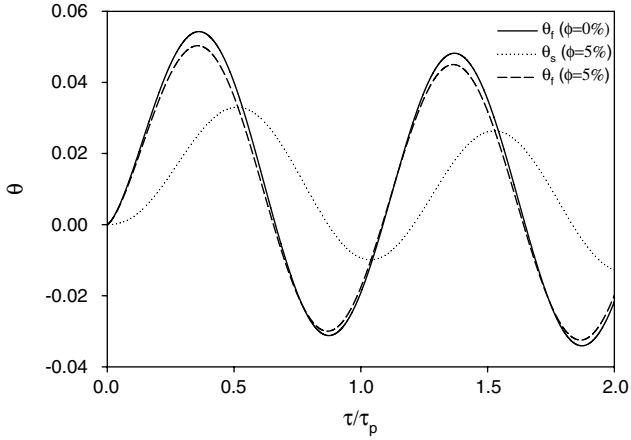

(b) $\tau_p = 0.01$

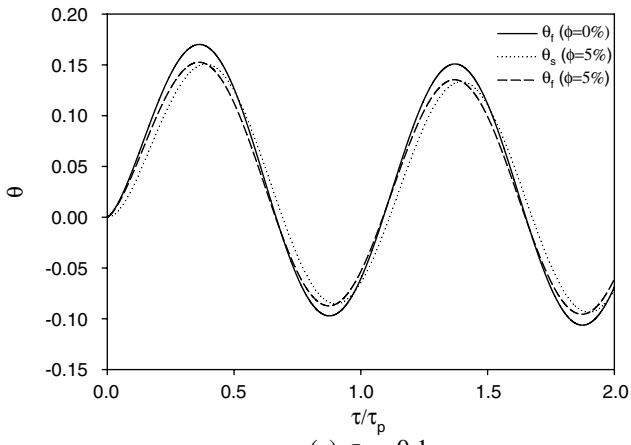

(c) $\tau_p = 0.1$

Fig. 7. Surface temperature for diamond–EG nanofluid ($C_{sf} = 2.728$, $Sp = 1000$, $\varphi = 5\%$).

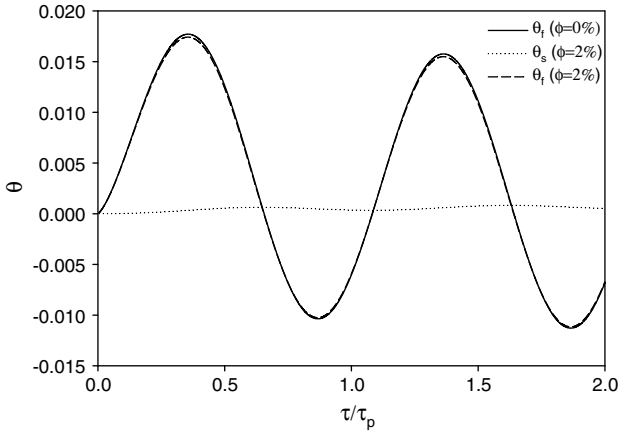

(a) $\tau_p = 0.001$

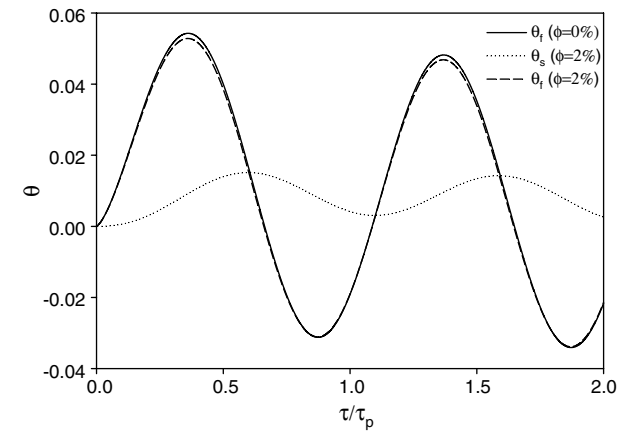

(b) $\tau_p = 0.01$

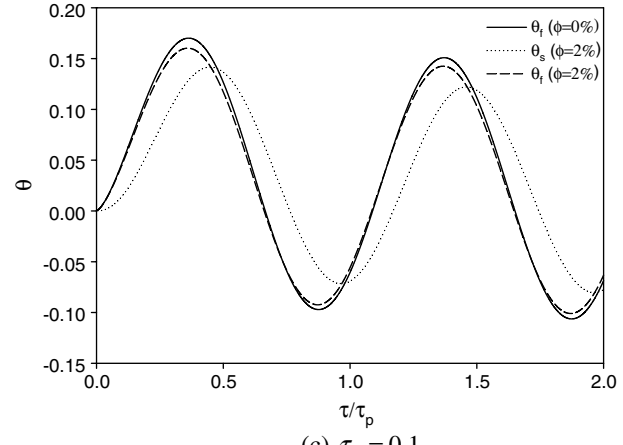

(c) $\tau_p = 0.1$

Fig. 8. Surface temperature for copper–EG nanofluid ($C_{sf} = 5.248$, $Sp = 500$, $\varphi = 2\%$).

Fig. 9. The amplitude of base fluid temperature oscillation noticeably decreases with increasing volume fraction of nanoparticle – an indication of heat transfer enhancement. The nonequilibrium phenomena in Fig. 9 are also more significant than those for the diamond–EG nanofluid shown in Fig. 6. The heat transfer enhancement parameter, Θ, for the three different periods of surface heat fluxes are 3.49%, 4.63% and 14.17%, respectively. Compared with the heat transfer enhancement parameter for $\varphi = 2\%$, the heat transfer enhancement parameter for all three periods of surface heat flux are significantly higher. Compared with the diamond–EG nanofluid, the heat transfer enhancement

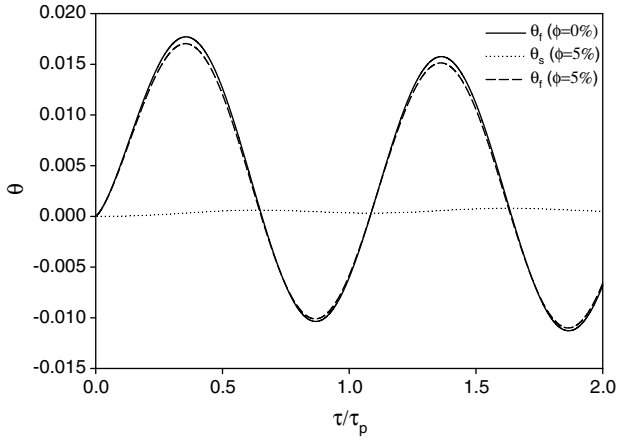

(a) $\tau_p = 0.001$

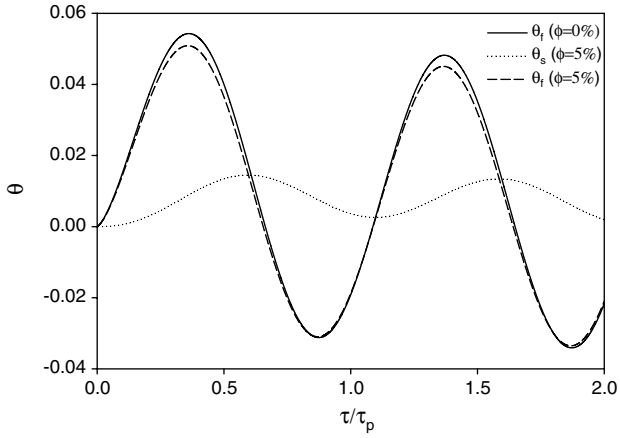

(b) $\tau_p = 0.01$

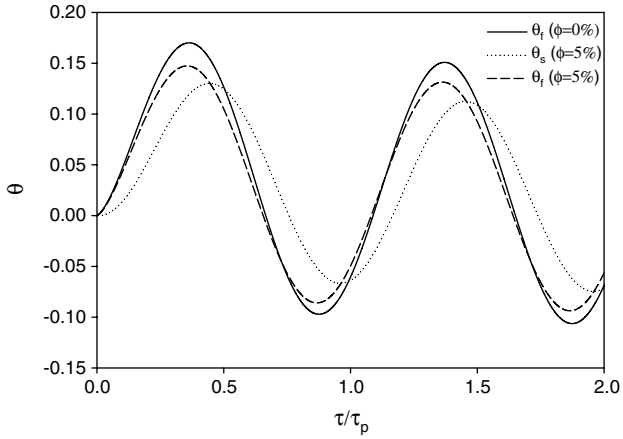

(c) $\tau_p = 0.1$

Fig. 9. Surface temperature for copper–EG nanofluid ($C_{sf} = 5.248$, $Sp = 500$, $\varphi = 5\%$).

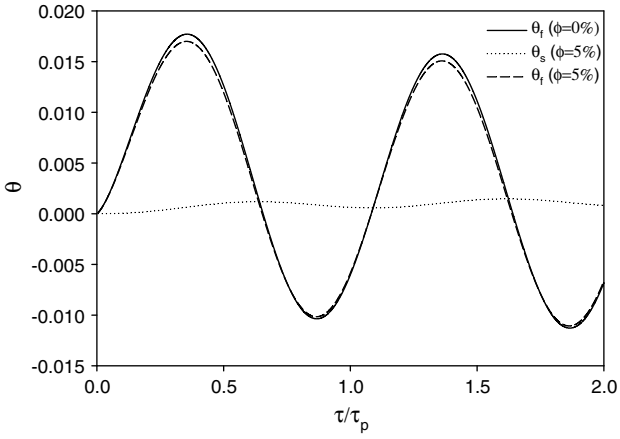

(a) $\tau_p = 0.001$

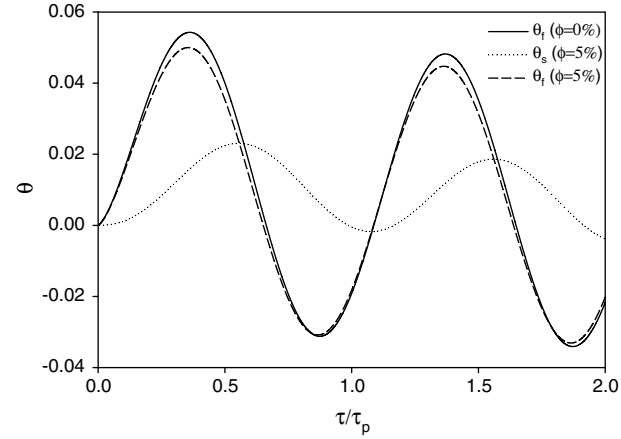

(b) $\tau_p = 0.01$

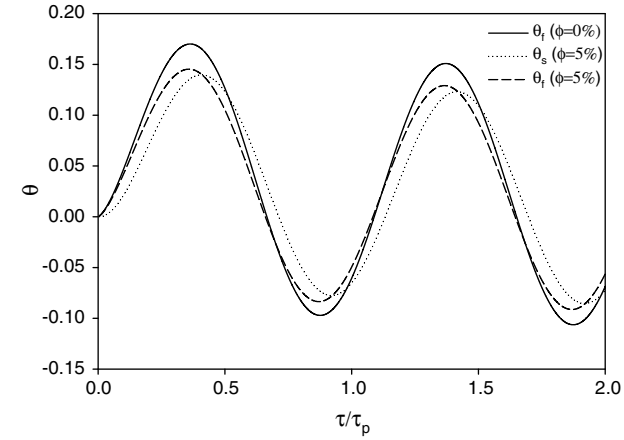

(c) $\tau_p = 0.1$

Fig. 10. Surface temperature for copper–EG nanofluid ($C_{sf} = 5.248$, $Sp = 1000$, $\varphi = 5\%$).

parameter for the copper–EG nanofluid did not show any meaningful difference.

The final simulation is performed for the copper–EG nanofluid for the cases with Sparrow number equal to 1000 and the results are shown in Fig. 10. As the Sparrow number is doubled compared to that of Fig. 9, the amplitudes of the temperature oscillation of nanoparticles increase while the amplitudes of the temperature oscillation of base fluid slightly decrease. The heat transfer enhancement parameter, Θ, for the three different periods of surface heat fluxes are 3.49%, 5.45%, and 16.69%, respectively. The Sparrow number did not have a significant effect on the heat transfer enhancement parameter.

5. Conclusions

Heat conduction in a nanofluid layer with periodic heat flux on one side and specified temperature on the other side is investigated. The effects of heat capacity ratio, volume fraction of nanofluid, Sparrow number, and the period of surface heat flux on nonequilibrium and heat transfer enhancement were investigated. The results showed that the nonequilibrium and heat transfer enhancement in the nanofluid are significantly affected by the heat capacity ratio between the nanoparticles and the base fluid, while the thermal conductivity of nanoparticle material is irrelevant for nonequilibrium and heat transfer enhancement. Increasing heat capacity ratio causes decreasing amplitude of nanoparticle temperature oscillation because the same level of energy exchange between the nanoparticles and base fluid results in less change on the nanoparticle temperature for large heat capacity ratio. The nonequilibrium is more significant with higher heat capacity ratio, higher volume fraction of nanoparticles, lower Sparrow number, and shorter periods of surface heat flux. The enhancement of heat transfer improves with increasing heat capacity ratio, volume fraction of nanoparticles, Sparrow number, and the period of surface heat flux.

The maximum heat transfer enhancement in this paper is 16.7% obtained for copper–EG nanofluid with 5% of nanoparticles; this enhancement is much lower than those obtained using transient hot wire (THW) method, but consistent with the latest experimental results obtained with optical beam deflection technique [25]. It should be pointed out that the results presented in this paper is based upon assumption that there is no direct interaction between nanoparticles [see Eq. (1)]. Collisions, clustering and aggregation of nanoparticles may cause direct interaction of nanoparticles which are not taken into account in this paper. The thermal diffusion of nanoparticles in the nanofluid layer with temperature gradient that could contribute to the heat transfer enhancement is also not taken into account. Further efforts with these effects accounted for will be essential to uncover the heat transfer mechanisms in the nanofluid.

Acknowledgements

The authors would like to express their gratitude to Dr. Robert D. Tzou for his valuable discussions. The work presented in this article was funded by the Office of Naval Research Grant No. N00014-06-1-1119, under the direction of Dr. Mark Spector.

References

[1] S.U.S. Choi, Enhancing thermal conductivity of fluids with nanoparticles, developments and applications of non-newtonian flows, in: D.A. Siginer, H.P. Wang (Eds.), FED – vol. 231/MD – vol. 66, The American Society of Mechanical Engineers, New York, pp. 99–105.

[2] J.A. Eastman, S.U.S. Choi, S. Li, W. Yu, L.J. Thompson, Anomalously increased effective thermal conductivities of ethylene glycol-based nano-fluids containing copper nano-particles, Appl. Phys. Lett. 78 (2001) 718–720.

[3] S.U.S. Choi, Z.G. Zhang, W. Yu, F.E. Lockwood, E.A. Grulke, Anomalous thermal conductivity enhancement in nano-tube suspensions, Appl. Phys. Lett. 79 (2001) 2252–2254.

[4] S.K. Das, N. Putra, P. Thiesen, W. Roetzel, Temperature dependence of thermal conductivity enhancement for nanofluids, ASME J. Heat Transfer 125 (2003) 567–574.

[5] H.E. Patel, S.K. Das, T. Sundararajan, A.S. Nair, B. George, T. Pradeep, Thermal conductivities of naked and monolayer protected metal nanoparticle based nanofluids: manifestation of anomalous enhancement and chemical effects, Appl. Phys. Lett. 83 (2003) 2931–2933.

[6] J.A. Eastman, S.R. Phillpot, S.U.S. Choi, P. Keblinski, Thermal transport in nanofluids, Annu. Rev. Mater. Res. 34 (2004) 219–246.

[7] S.K. Das, S.U.S. Choi, H.E. Patel, Heat transfer in nanofluids – a review, Heat Transfer Eng. 27 (2006) 3–9.

[8] P. Keblinksi, S.R. Phillpot, S.U.S. Choi, J.A. Eastman, Mechanisms of heat flow in suspensions of nano-sized particles (nanofluids), Int. J. Heat Mass Transfer 45 (2002) 855–863.

[9] D.H. Kumar, H.E. Patel, V.R.R. Kumar, T. Sundararajan, T. Pradeep, S.K. Das, Model for heat conduction in nanofluids, Phys. Rev. Lett. 93 (2004) 144301.

[10] P. Keblinski, D.G. Cahill, Comment on "model for heat conduction in nano fluids", Phys. Rev. Lett. 95 (2005) 209401.

[11] S.P. Jiang, S.U.S. Choi, Role of Brownian motion in the enhanced thermal conductivity of nanofluids, Appl. Phys. Lett. 84 (2004) 4316–4318.

[12] R. Prasher, P. Bhattacharya, P.E. Phelan, Thermal conductivity of nanoscale colloidal solutions (nanofluids), Phys. Rev. Lett. 94 (2005) 025901.

[13] W. Evans, J. Fish, P. Keblinski, Role of Brownian motion hydrodynamics on nanofluid thermal conductivity, Appl. Phys. Lett. 88 (2006) 093116.

[14] Q. Xue, Model for effective thermal conductivity of nanofluids, Phys. Lett. A 307 (2003) 33–317.

[15] Q. Xue, W.M. Xu, A model of thermal conductivity of nanofluids with interfacial shells, Mater. Chem. Phys. 90 (2005) 298–301.

[16] W. Yu, S.U.S. Choi, The role of interfacial layers in the enhanced thermal conductivity of nanofluids: a renovated Maxwell model, J. Nanoparticle Res. 5 (2003) 167–171.

[17] W. Yu, S.U.S. Choi, The role of interfacial layers in the enhanced thermal conductivity of nanofluids: a renovated Hamilton–Crosser model, J. Nanoparticle Res. 6 (2004) 355–361.

[18] K.C. Leong, C. Yang, S.M.S. Murshed, A model for the thermal conductivity of nanofluids – the effect of interfacial layer, J. Nanoparticle Res. 8 (2006) 245–254.

[19] C.J. Yu, A.G. Richter, A. Datta, M.K. Durbin, P. Dutta, Molecular layering in a liquid on a substrate: an X-ray reflective study, Physica B 283 (2000) 27–31.

[20] L. Xue, P. Keblinski, S.R. Phillpot, S.U.S. Choi, J.A. Eastman, Effect of liquid layering at the liquid–solid interface on thermal transport, Int. J. Heat Mass Transfer 47 (2004) 4277–4284.

[21] Y. Xuan, Q. Li, W. Hu, Aggregation structure and thermal conductivity of nanofluids, AIChE J. 49 (2003) 1038–1043.

[22] B.X. Wang, L.P. Zhou, X.F. Peng, A fractal model for predicting the effective thermal conductivity of liquid with suspension of nanoparticles, Int. J. Heat Mass Transfer 46 (2003) 2665–2672.

[23] P. Vadasz, Heat conduction in nanofluid suspensions, J. Heat Transfer 128 (2006) 465–477.

[24] D.Y. Tzou, Macro- to Microscale Heat Transfer – The Lagging Behavior, Taylor & Francis, Bristol, PA, 1997.

[25] S.A. Putnam, D.G. Cahill, P.V. Braun, Z. Ge, R.G. Shimmin, Thermal conductivity of nanoparticle suspensions, J. Appl. Phys. 99 (2006) 084308-1–084308-3.

[26] Y. Zhang, A. Faghri, Advances and unresolved issues in pulsating heat pipes, Heat Transfer Eng. 29 (1) (2008) 20–44.

[27] Y. Zhang, A. Faghri, Heat transfer in a pulsating heat pipe with open end, Int. J. Heat Mass Transfer 45 (2002) 755–764.
[28] H.B. Ma, B. Bogmeyer, C. Wison, H. Park, Q. Yu, M. Tirumala, S. Choi, Nanofluid effect on the heat transport capability in an oscillating heat pipe, Appl. Phys. Lett. 88 (1–3) (2006) 143116-1–143116-3.
[29] H.B. Ma, C. Wilson, Q. Yu, U.S. Choi, M. Tirumala, An experimental investigation of heat transport capability in a nanofluid oscillating heat pipe, ASME J. Heat Transfer 128 (2006) 1213–1216.
[30] Y. Zhang, Nonequilibrium modeling of heat transfer in a gas-saturated powder layer subject to short-pulsed heat source, Numer. Heat Transfer, Part A 50 (2006) 509–524.
[31] H.E. Patel, T. Sundararajan, S.K. Das, A cell model approach for thermal conductivity of nanofluids, J. Nanoparticle Res. 10 (2008) 87–97.
[32] W.J. Minkowycz, A. Haji-Sheikh, K. Vafai, On departure from local thermal equilibrium in porous media due to a rapidly changing heat source: the Sparrow number, Int. J. Heat Mass Transfer 42 (1999) 3373–3385.
[33] S.A. Putnam, D.G. Cahill, B.J. Ash, L.S. Schadler, High-precision thermal conductivity measurements as a probe of polymer/nanoparticle interface, J. Appl. Phys. 94 (2003) 6785–6788.
[34] A.M. Al-Amiri, Natural convection in porous enclosures: the application of the two-energy equation model, Numer. Heat Transfer, Part A 41 (2002) 817–834.
[35] S. Krishnan, J.Y. Murthy, S.V. Garimella, A two-temperature model for the analysis of passive thermal control systems for electronics, ASME J. Heat Transfer 126 (2004) 628–637.
[36] D.Y. Tzou, Computational Technique for Microscale Heat Transfer, Handbook of Numerical Heat Transfer, John Wiley & Sons, Hoboken, NJ, 2006, pp. 623–658.
[37] S.V. Patankar, Numerical Heat Transfer and Fluid Flow, McGraw-Hill, New York, 1980.